

A Functionally Graded Syntactic Foam Material for High Energy Absorption under Compression

Nikhil Gupta

Composite Materials and Mechanics Laboratory
Mechanical, Aerospace and Manufacturing Engineering Department
Polytechnic University, Brooklyn, NY 11201
Phone: 718-260 3080, Fax: 718-260 3532
Email: ngupta@poly.edu

Abstract

A functionally graded structure for hollow particle (microballoon) filled syntactic foams is fabricated that is capable of withstanding compression for 60-75% strain without any significant loss in strength. The new functionally graded structure is based on creating a gradient in microballoon wall thickness. This material has the same volume fraction of microballoons throughout the structure, eliminating the undesirable effects of the present functionally graded composites containing a gradient of particle volume fraction. Three compositions of such material are fabricated and tested in the present study. Results show that the compressive modulus, strength, and total energy absorption of the new syntactic foams can be controlled by using appropriate type and volume fraction of microballoons.

Keywords: composite materials, mechanical properties, syntactic foam, porosity, microballoon, functionally graded material.

Introduction

Syntactic foams, which are hollow particle (microballoon) filled composites, can be found studied for aerospace applications [1, 2]. Compressive and high strain rate properties of these foams are widely studied in the published literature [3-6]. Syntactic foams show a stress-plateau in their compressive stress-strain curves as shown in Figure 1, which represents their energy absorption characteristics [3, 4]. Lower density foams show a larger stress plateau but lower strength compared to higher density foams [3]. Several techniques such as variation in type and volume fraction of microballoons (V_{mb}) and matrix plasticization by means of fillers have been studied with limited success in further elongating the plateau region [7]. Syntactic foams can be found studied in functionally graded structure also. The presently available functionally graded syntactic foams (FGSFs) are synthesized by creating a gradient of V_{mb} along one dimension of the material structure [8-11]. However, the energy absorption under compressive loading conditions is not found to be significantly improved in these FGSFs. Changing V_{mb} causes non-uniform stress concentrations in the material, which may cause catastrophic failure originating in the matrix rich side of the specimen, especially when the matrix is a brittle polymer such as epoxy resins. There are additional disadvantages associated with such FGSFs. Varying volume fractions of microballoons and

matrix across the thickness cause a gradient in the coefficient of thermal expansion and moisture absorption. This results in warping, leading to instability, when the material is exposed to changing temperature or moisture conditions. The approach also poses severe limitations on the minimum density achievable in such materials, especially when the filler particles have lower density than the matrix resin. The present study is based on fabricating a FGSF with high energy absorption capabilities under compressive loading conditions. Other limitations of the present FGSFs can also be overcome if the new structure is independent of volume fraction gradient.

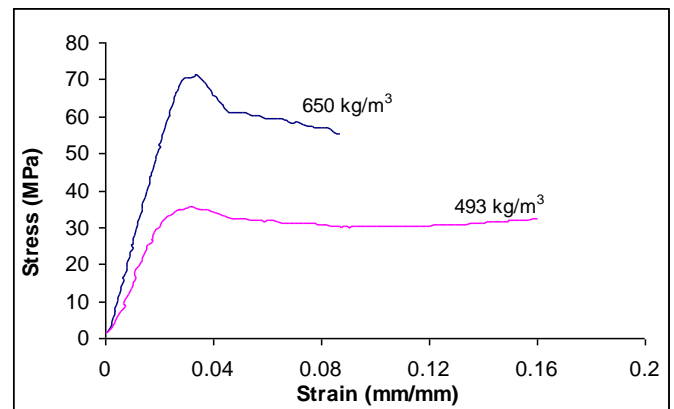


Fig. 1. Compressive stress-strain curves for plain syntactic foams having two different densities.

For microballoons a parameter named Radius Ratio (η) is defined as Equation 1, which relates the microballoon wall thickness to its size [3]:

$$\eta = \frac{r_i}{r_o} \quad (1)$$

where r_i and r_o are the inner and outer radii of the microballoon. A higher value of η leads to a lower wall thickness in the same size microballoons and results in lower strength. Previous experimental studies have observed that the strength and modulus of syntactic foams increase linearly with decrease in microballoon η [12]. The FGSF studied in this research takes advantage of the possibility of creating a gradient of η , while keeping the V_{mb} constant. A schematic of the specimen composition and compression test scheme are presented in Figure 2a and the material microstructural representation is shown in Figure 2b. Each layer of the material in Figure 2a contains the same V_{mb} .

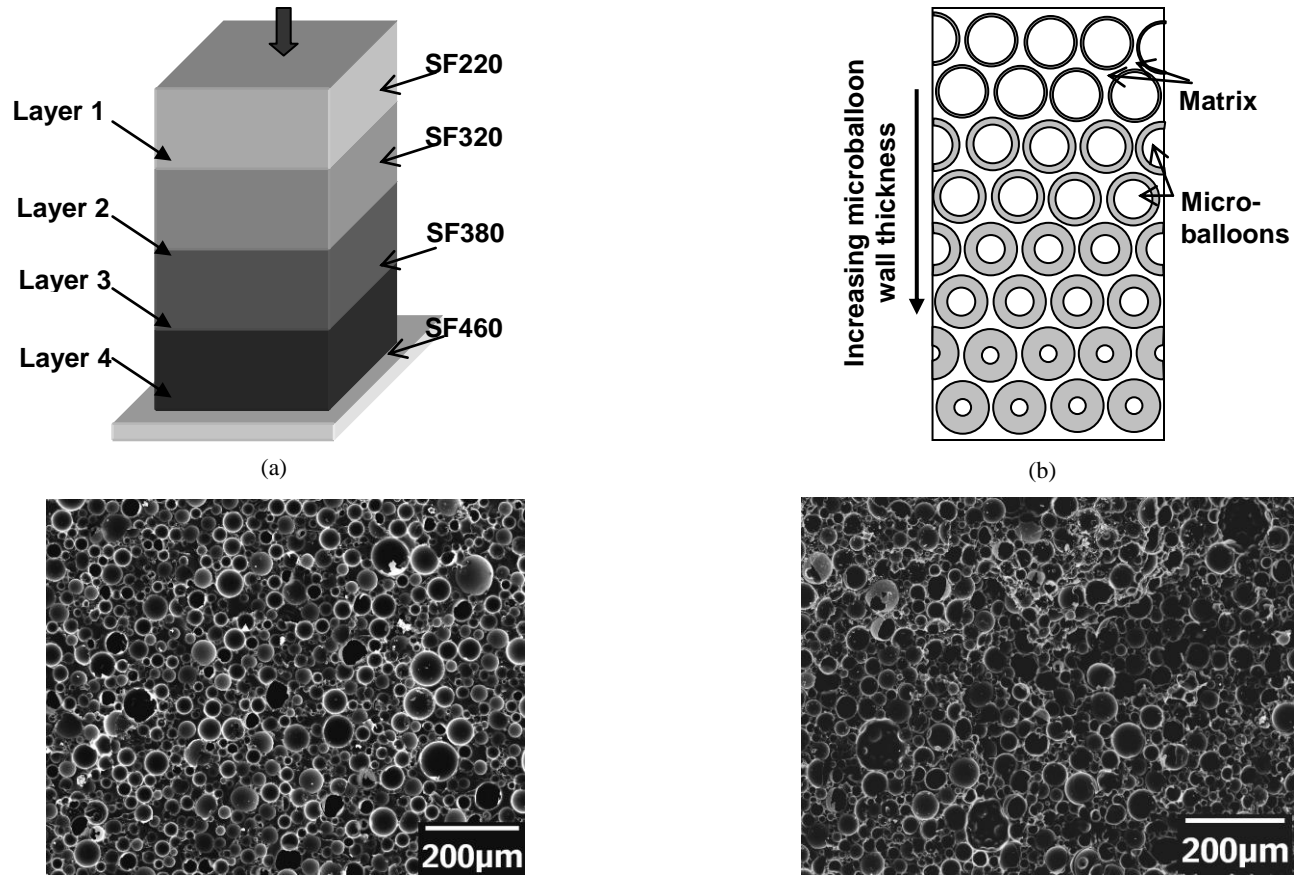


Fig. 2. (a) Schematic representation of specimen structure and (b) microstructure; scanning electron micrograph of syntactic foams of (c) SF220 and (d) SF460 type having 60% microballoons by volume.

Hence, the V_{mb} remains the same throughout the structure but difference in the microballoon η leads to generation of functionally graded structure. The micrographs for syntactic foam containing the same V_{mb} of different types of microballoons would appear to be similar because microballoons of the same outer diameters are used in each layer. SF220 and SF460 foams containing V_{mb} of 0.6 are shown in Figures 2c and 2d for comparison. However, values of their densities would provide an evidence of having a gradient in η .

Materials and Experimental Methods

Four types of Scotchlite™ glass microballoons, manufactured and supplied by 3M, are used in three volume fractions (0.5, 0.6 and 0.65) to synthesize twelve types of syntactic foams. The size, density and calculated η for microballoons used in synthesis of these foams are given in Table 1. The notations for syntactic foam type in Table 1 are related to the true particle density of microballoons used in syntactic foams. The average outer diameter of all types of microballoons is nearly the same and the only difference is in their wall thickness (or η). DOW manufactured DER 332 Epoxy resin with Hardener DEH 24 and diluent C₁₂-C₁₄ aliphaticglycidylether, are used as the matrix material. All constituent materials were mixed and cured at room temperature for 24 h and then post cured at 100°C for 3 h. Syntactic foam chips of 12×12×5 mm³ were sectioned and bonded together with thin layers of an epoxy based adhesive to fabricate FGSFs similar to those shown in Figure 2a.

Table 1. Properties of microballoons used in the study.

Syntactic Foam Type	Average Microballoon Size (µm)	True Particle Density (kg/m ³)	Radius Ratio η
SF220	35	220	0.9703
SF320	40	320	0.9561
SF380	40	380	0.9474
SF460	40	460	0.9356

The theoretical and measured densities and porosities for all types of syntactic foam are given in Table 2. The total porosity in syntactic foams (V_t) can be estimated as a sum of the closed cell porosity entrapped inside microballoons and the matrix porosity.

$$V_t = V_{mb} \times \eta^3 + \frac{\rho_{th} - \rho_m}{\rho_{th}} \quad (2)$$

where ρ_{th} and ρ_m are the theoretical density calculated using Rule of Mixtures and the measured density of syntactic foams, respectively. The first term on the right side in Equation 2 represents the porosity enclosed within microballoons, termed as microballoon porosity, and the second term is the porosity embedded in the matrix between microballoons, termed as matrix porosity.

Four specimens of each type of FGSF were prepared and tested under the compression rate of 1 mm/min. The tests were stopped when the densification of the material was completed and the stress-plateau region ended

Table 2. Density of syntactic foam layers and functionally graded syntactic foams and porosity estimates.

FGSF Type	V_{mb}	Layer #	Foam Type	Theoretical Density (kg/m ³)	Microballoon Porosity (%)	Matrix Porosity %	Measured Density (kg/m ³)	Total Porosity in FGSF (%)	Density of FGSF (kg/m ³)
1	0.50	1	SF220	690	45.7	11	611	43.2	677
		2	SF320	740	43.7	9	670		
		3	SF380	770	42.5	10	694		
		4	SF460	810	40.9	10	732		
2	0.60	1	SF220	596	54.8	8	550	51.8	608
		2	SF320	656	52.4	7	611		
		3	SF380	692	51.0	10	625		
		4	SF460	740	49.1	12	645		
3	0.65	1	SF220	549	59.4	8	504	56.2	572
		2	SF320	614	56.8	11	543		
		3	SF380	653	55.3	10	588		
		4	SF460	705	53.2	7	654		

Results and Discussion

The representative compressive stress-strain curves for the three types of FGSFs are shown in Figure 3, which can be compared with those of the plain syntactic foams shown in Figure 1. It is observed that the stress-plateau region extends to over 60% strain for all FGSFs. An increase from less than 20% to over 60% in the stress-plateau region significantly improves the energy absorption characteristics and makes them highly damage tolerant. At the end of the stress-plateau the densification completes and stress starts rising again, which is similar to plain syntactic foams. Hence, these materials do not show any specific fracture point in their entire length of stress-strain curve for over 70% strain.

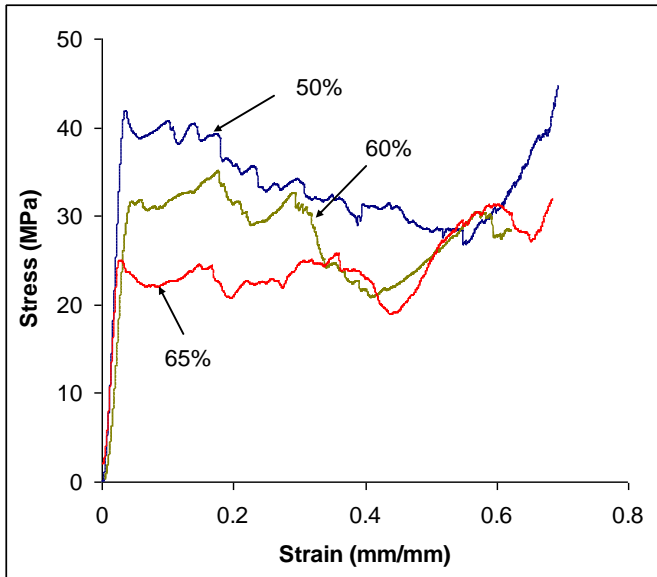


Fig. 3. Compressive stress-strain curves for FGSFs containing 65%, 60% and 50% microballoons by volume.

The modulus and strength of FGSFs depend on the weakest layer, which fails first, defining the strength and modulus of the material. The modulus and strength of each layer is determined by the strength and volume fraction of matrix and microballoons present in that layer. In the present case the weakest layer is SF220, which contains microballoons of highest η . Properties of matrix material and V_{mb} are the

same in various layers of foams in one type of FGSF and the only difference is the microballoon η . Hence, the FGSF strength and modulus are directly dependent on the radius ratio of microballoons present in the weakest layer, SF220. Calculated from the stress-strain curves, the compressive modulus values are 1134, 1344 and 1440 MPa for FGSFs having V_{mb} of 65%, 60% and 50%, respectively. The corresponding compressive yield strength values are 23.7, 32.7 and 41 MPa. These values are very close to the modulus and strength values of SF220 syntactic foam [3].

The fracture pattern of FGSFs is shown in Figure 4. In Figure 4a initiation of cracks can be observed in SF220 and SF320 layers, which contain weaker microballoons of higher η . On further compression SF220 layers is completely crushed (Figure 4b). Once the densification of the weakest layer completes the stress starts increasing and the next layer starts deforming, which sometimes causes appearance of a small peak in the stress-strain curve. The crack initiation in higher density layers under the effect of secondary tensile stresses causes their failure at lower stress but contributes in elongating the stress-plateau. It can be observed in Figure 3 that with increase in V_{mb} the stress-plateau becomes more stable. Such a trend is observed because with decreasing volume fraction of resin the effect of cracks originated in the resin becomes less significant. In specimens containing V_{mb} of 0.5 the stress shows a gradual decreasing trend from about 20% to 55% strain. However, even at 55% strain the stress is decreased by about 30% only. The strain for complete densification depends on the total porosity in the foam specimens defined by Equation 2. In specimens containing V_{mb} of 0.5 and 0.65 the total porosity volumes are 53% and 65%, respectively (Table 2). Hence, it is possible to obtain the compressive strain in this range. However, the unrestricted lateral expansion under the standard test conditions also contributes in elongating the stress plateau region. Hence, a combined effect of these factors appears as 60-75% strain till the densification completes. The average plateau stress for the FGSFs containing V_{mb} of 0.65, 0.6 and 0.5 is found to be 23, 29 and 37 MPa, respectively. It is noticed that the stress is constant within a narrow band in the plateau region and there is no visible sign of specimen failure. Hence, the use of FGSFs may enhance the structural safety and reliability.

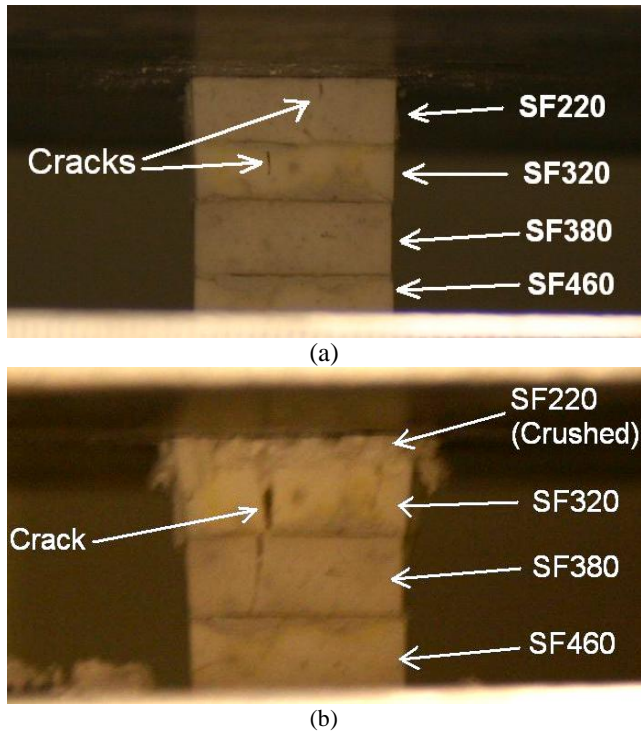


Fig. 4. During compression of FGSF (a) initiation of cracks in weaker layers and (b) complete crushing of weakest SF220 (top layer) layer while cracks initiate in the second and the third layers. The bottom layer, the strongest one, is still undeformed.

The total energy absorption in compression can be estimated in terms of the area under the stress-strain curve. In plane syntactic foams the area under the curves is on the order of 3-6 MPa [7], whereas in FGSFs, it is measured to be 16, 16.5 and 21 MPa for 0.65, 0.6 and 0.5 V_{mb} specimens. The energy absorption is higher for specimens having 0.5 V_{mb} because of higher strength of these specimens. Based on the results it can be observed that the total energy absorbed in FGSFs can be changed by changing V_{mb} . Since, the energy absorption characteristics are also related to the strength and modulus of the composite, a combination of these three parameters needs to be considered while preparing or selecting appropriate FGSF for a given application.

The present study demonstrates a microstructure of FGSF that is found to be more energy absorbent compared to other syntactic foams. Further enhancement in properties can be achieved by selecting microballoons of different material or a different matrix resin. Metal matrix syntactic foams are also being studied by several researchers [13, 14]. Such microstructures can be created in metal matrix syntactic foams also. Several material parameters such as V_{mb} and η of microballoons used in various layers and thickness of each layer can be optimized to create a FGSF with pre-specified strength, modulus and densification strain.

Conclusions

The study presents the concept of a novel FGSF microstructure based on microballoon η and characterizes three variations of such FGSFs fabricated in layered structure. The FGSF is found to be capable of withstanding 60-75% compression, depending on the composition, without any significant loss in strength or failure. The compressive strength and modulus of FGSFs are found to be dependent on those of the weakest layer in their structure. The area under the stress-strain curves is found to be 300-500% higher compared to plain syntactic foams, indicating significantly higher energy absorption in these FGSFs. It would be of great interest to synthesize FGSFs with such structures in a single material with smooth gradient in microballoon η and mechanical properties instead of having layered structure.

Acknowledgments

The author wishes to thank 3M for providing microballoons and relevant technical information. Extensive help of William Ricci in specimen preparation and testing is sincerely acknowledged. The author thanks Alessandro Betti for help in specimen cutting and polishing. Partial funding for the research was provided by Othmer Institute, which is gratefully acknowledged.

References

1. A.J. Hodge, NASA Technical Report NASA/TM—2000—210252.
2. M. Suits, NASA Technical Report: NASA/TM—1999—209148.
3. N. Gupta, E. Woldesenbet, P Mensah, Composites Part A 35 (2004) 103.
4. N. Gupta, Kishore, E. Woldesenbet, S. Sankaran, J Mater Sci 36 (2001) 4485.
5. D. Rittel, Materials Letters, 59, 14-15 (2005) 1845.
6. P. R. Marur, Materials Letters, 59 (2005) 1954.
7. N. Gupta, R. Maharsia, H.D. Jerro, Mater Sci Eng A 395 (2005) 233.
8. Kishore, R. Shankar and S. Sankaran, Mat Sci Eng A 412 (2005) 153-158.
9. V. Parameswaran, A. Shukla, J Mater Sci 35 (2000) 21.
10. V. Parameswaran, A. Shukla, Mech Res Commun 29 (2002) 397.
11. M.A. El-Hadek, H.V. Tippur, Int J Sol Struct 40 (2003) 1885.
12. N. Gupta, E. Woldesenbet, J Cell Plast 40 (2004) 461.
13. D. K. Balch, J. G. O'Dwyer, G. R. Davis, C. M. Cady, G. T. Gray III, D. C. Dunand, Mater Sci Eng A, 391 (1-2) (2005) 408.
14. P.K. Rohatgi, J.K. Kim, N. Gupta, Simon Alaraj and A. Daoud. Composites Part A, 37 (3) (2006) 430.